



# Influence of Cryogenic Treatment on Microstructure and Mechanical Properties of Ti6Al4V Alloy

Fatih Hayati Çakir and Osman Nuri Çelik

(Submitted July 1, 2020; in revised form September 18, 2020; accepted September 25, 2020; published online October 13, 2020)

Cryogenic treatment is an emerging application that can make significant changes in many materials. In this study, shallow ( $-80\text{ }^{\circ}\text{C}$ ) and deep ( $-196\text{ }^{\circ}\text{C}$ ) cryogenic treatment was applied to Ti6Al4V alloy. Additionally, aging treatment and supplementary deep cryogenic treatment were also performed. Tensile tests were done to observe the effects of cryogenic treatment on the mechanical properties and formability of Ti6Al4 alloy. According to the results of these tests, it was observed that the cryogenic treatment had a positive influence on the plasticity properties of Ti6Al4V alloy. For the 24-h and 36-h deep cryo-treated samples, the uniform plastic deformation region (UPDR) was extended 5 and 8.3% compared to untreated sample, respectively. However, this improvement in plasticity observed in samples treated with cryogenic treatment for 36 h led to a decrease in yield strength by 2%. Microstructural and XRD analysis was performed to characterize the microstructural changes that happened with the effect of applied heat treatments. The characterization study shows that with the application of cryogenic treatment internal structure of the material changed, the  $\beta$  phase ratio of the alloy decreased from 8.1 to 5.6% with 36-h deep cryogenic treatment. The unstable  $\beta$  phase was transformed into  $\alpha$  phase and stable  $\beta$  phase. The experimental study shows that cryogenic treatment improves the plasticity and toughness of Ti6Al4V alloy at room temperature and regulates the microstructure and reduces the residual stress.

**Keywords** characterization, cryogenic treatment, mechanical properties, Rietveld analysis, Ti6Al4V, XRD

## 1. Introduction

Heat treatment is an effective way to tailor material properties for desired applications. There are many traditional heat treatment procedures for titanium alloys. The advantages and disadvantages of these procedures are mostly known. In the literature, there are many studies about the effect of traditional heat treatments on titanium alloys such as annealing, quenching aging on mechanical properties; however, the studies about the cryogenic treatment of titanium alloys are limited. Hence, the cryogenic treatment is a relatively new method. Cryogenic treatment is generally applied as additional heat treatment to parts in near-final shape. This sub-zero treatment generally takes long soaking times that might alter the microstructure and mechanical properties. Since the applied heat treatment affects the  $\alpha/\beta$  phase ratio, shape, and distribution of phases in the structure, it can be said that mechanical properties are also significantly affected by the application of heat treatments. In the study of Gu et al., the effects of cryogenic treatment on the plastic properties of Ti6Al4V alloy at room temperature and static conditions were investigated. The first group of specimens were soaked  $-196\text{ }^{\circ}\text{C}$  for 12 h, and another group was

cryo-treated and tempered at  $180\text{ }^{\circ}\text{C}$  for 3 h. It has been reported that the unstable  $\beta$  phase was transformed into  $\alpha$  phase and stable  $\beta$  phase by the effect of cryogenic treatments, and this finding is based on SEM images. Additionally, tensile tests were conducted, and it has been reported that cryogenic treatment decreases yield and tensile strength by approximately 25 MPa but increases elongation by 10.6% and reduction of the area by 13.5% (Ref 1). In another study, the effects of cryogenic treatment and the aging on Ti6Al4V material were investigated. A tensile test and microstructure analysis were performed in this study. Experimental groups include cryogenic treated and aged titanium alloys; however, solution treatment and quenching were not applied to aged samples. Results of the study show that plastic forming ability is improved in both cryogenic treatment when it was applied alone and with aging. The reason for this change was ground on the transformation of the semi-stable  $\beta$  phase to the stable  $\beta$  phase and the  $\alpha$  phase. According to the transmission electron microscopy (TEM) analysis, the cryogenic treatment affects the dislocation network, especially in the aging process following the cryogenic process; it is stated that it increases the density of dislocation and causes twin formation in the microstructure (Ref 2).

The changes that happened in the internal structure with heat treatment should be investigated in detail. One of the main approaches is optical and scanning electron microscope analysis. Another fundamental approach used for the characterization of titanium alloys is x-ray diffraction (XRD). Most of the studies conducted in the literature are conducted at room temperature. The XRD measurements with high temperature and in situ measurements are more limited (Ref 3). Sha and Malinov applied different heat treatments to Ti6Al4V alloy and carried out XRD analyses of the structures resulting from these heat treatments. In the literature, there are many various studies, which focus on different heat treatments of titanium alloys. The generated structures were examined by XRD analysis. XRD

Fatih Hayati Çakir, Eskişehir Vocational School, Eskişehir Osmangazi University, Eskişehir, Turkey; and Osman Nuri Çelik, Department of Mechanical Engineering, Eskişehir Osmangazi University, Eskişehir 26480, Turkey. Contact e-mails: fcakir@ogu.edu.tr and oncelik@ogu.edu.tr.

patterns were analyzed, and lattice dimensions were measured; the intensity and position of the peaks were analyzed and evaluated (Ref 4-8). In titanium alloys, the transformation of the  $\beta$  phase to the  $\alpha$  phase occurs in a mono-variant manner, and  $\alpha$  and  $\beta$  phases are balanced with different ratios at different temperatures. In continuous cooling, different phases of the  $\alpha$  phase can be precipitated. The thin-laminated structure is observed at transformations that occur at lower temperatures. In this case, the residual stress amounts of the  $\alpha$  phases precipitated at different temperatures also differ. The amount of alloying elements contained in the  $\alpha$  phase formed under different conditions is also different in certain proportions. The composition and the heat treatment of the Ti alloy affect the lattice parameters. XRD analysis of titanium materials is affected by materials' heat treatment history and the production method. Zeng and Bieler applied different heat treatments to titanium alloy. Ti6Al4V wire was cold drawn and aged in their study. Different phases ( $\alpha'$ ,  $\alpha'$ ,  $\alpha$ ,  $\beta$ ,  $\omega$ ) were observed with different processes. Different treated Ti6Al4V alloys were characterized, different phases were detected, lattice parameters of these phases are given. Although it is useful in terms of the location of phase transformations and peaks, the phase ratios of different structures obtained as a result of different processes are not included in the study (Ref 4). In another study, the Ti6Al4V alloy was heated to the  $\beta$  phase zone and then quenched. The quenching media were prepared in different hydrogen ratios. The resulting structures were analyzed by using the XRD technique. Transformation of  $\beta$  to  $\alpha$  in Ti6Al4V alloy is modeled using differential scanning calorimetry techniques. Differential cooling rates varying from 5 °C to 50 °C/min were used in the study. The experimental data obtained in this study were modeled mathematically, and the effect of cooling rate on phase transformation was investigated. The study was supported by XRD analysis, and continuous cooling (CCT) and time temperature conversion (TTT) diagrams were proposed (Ref 9). In situ XRD measurements are a very useful technique for observing the transformation of phases. Elmer et al. conducted in situ x-ray diffraction measurements in a heating state of Ti6Al4V to observe  $\alpha \rightarrow \beta$  phase transformation. Lattice parameters and phase transformations were observed in the study with different heating rates. It was stated that residual stress should be taken into consideration for conducting accurate analysis (Ref 6). In another study, Jovanović et al. investigated Ti6Al4V alloys produced by the investment casting method were annealed at different temperatures and investigated the structures obtained by using different cooling rates. In their study, the Ti6Al4V alloys were annealed at 800, 850, 900, 950, 1000, 1050, 1100 °C for 1 h and then, they examined these structures by cooling them in air and water using metallography, mechanical tests and XRD technique (Ref 10).

One of the well-known applications to harden Ti6Al4V alloy is aging. The outcomes of the aging process are strongly related to initial heat treatment conditions, aging temperature, and duration. Besides the generic approach, one of the recent studies reported that the best previous microstructure to benefit from aging is martensitic structure, but the best response to aging in terms of hardness increase was shown in conditions with globular, Widmanstätten, and bimodal microstructures with a higher content of  $\beta$  phase. The study suggests that at the correct temperature (500 °C) and duration (24 h), the formation

of Ti<sub>3</sub>Al is possible and increases the hardness more (Ref 11). In addition to heat treatment, the titanium alloys microstructure and mechanical properties can also be altered by mechanical and thermo-mechanical treatment (Ref 12). The deformation temperature plays a significant role in recovery, breakage, and globularization, but also the decomposition of  $\alpha$  and  $\beta$  phases.

Since the cryogenic treatment occurs at low temperatures, the molecular movements at that level are limited, that is why long treatment durations such as 24 h-36 h are used to benefit from cryogenic treatment. This duration is strongly affected by material type and heat treatment conditions. Previous studies show that there is an optimum soaking duration for the desired outcome. For instance, Gunes et al. applied the cryogenic treatment to 52,100 bearing steel at -145 °C with different soaking times (12, 24, 36, 48, 60 h) and stated that the optimum duration was 36 h to maximize the wear resistance (Ref 13). Additionally, tempering is suggested after cryogenic treatment in many studies (Ref 14). Additionally, cryogenic treatment is also reported to improve the machinability (Ref 15) and formability (Ref 1). The reported improvements were mostly grounded on the refinement of internal structure, decrease in internal residual stress, and improvement of electrical conductivity (Ref 16). These effects were also reported for cutting tool materials such as WC-Co (Ref 17).

Many studies report that cryogenic treatment increases electrical conductivity by regulating dislocations and in many materials. In the literature, there are many studies of cryo-treated ferrous (Ref 18-21) and non-ferrous (Ref 22-24) alloys, which claimed to benefit from controlled, cryogenic treatment. Reported studies and mechanisms about cryogenic treatment show that cryogenic treatments can make changes in many materials. However, cryogenic treatment of Ti6Al4V alloys and its effects were not investigated in detail regarding its effect on microstructure and mechanical properties. The previous studies were not focused on detailed characterization by using the XRD technique. With the help of prior studies and experimental work conducted, a more comprehensive analysis is presented. In this study, the effects of different cryo-treatment procedures on mechanical properties were investigated and reported. Additionally, the mechanisms of cryogenic treatment on titanium alloys were analyzed by optical microscope and XRD techniques. The mechanism of phase transformations induced by cryogenic treatment is explained.

## 2. Materials and Methods

Titanium alloy was supplied as sheet metal and cylindrical rod in ASTM B348 Grade 5 standard to examine the effect of the cryogenic treatment on the microstructure and mechanical properties of Ti6Al4V alloy. The Ti6Al4V alloy was annealed at 700 °C as supplied condition. Tensile test specimens were machined from sheet metal plates using the wire electrical discharge machining (WEDM) method. While performing these operations, process parameters were controlled to ensure that the effects of the sample preparation process did not affect the final product. All the tests were conducted and repeated three times under the same conditions. The conducted experimental study can be summarized as sample verification, heat treatment, microstructure analysis, XRD tests, and tensile tests.

## 2.1 Heat Treatment

Cryogenic treatment processes success and its effects are quite related to the initial state of the material. In this study, eight different groups of samples were prepared in 2 main categories. In total, 24 test samples were used to verify the test results. There were two main categories defined. First group deals with the effect of cryogenic treatment of annealed state Ti6Al4V alloys, which were designated to G2-G5. The second group was solution treated and aged designated as G6-G8. G1 was used as supplied state and used as the reference sample. G2 and G3 were cryo-treated at  $-80\text{ }^{\circ}\text{C}$  for 12 and 24 h, while G4 and G5 of samples were subjected to deep cryogenic treatment at  $-196\text{ }^{\circ}\text{C}$  for 24 and 36 h. The G6 was solution treated at  $920\text{ }^{\circ}\text{C}$  for 1 h and after that, quenched in an oil medium and then aged for 3 h at  $650\text{ }^{\circ}\text{C}$ , and the G7 and G8 were subjected to deep cryogenic treatment for 24 and 36 h after quenching prior to aging. Aging is the primary method to harden Ti6Al4V alloys with this approach; the effect of cryogenic treatment on the aging process was also made. G6, G7, and G8 samples were solutionized at  $920\text{ }^{\circ}\text{C}$  for 1 h; after that, samples were quenched to room temperature in oil medium, and then, G6 samples were directly aged at  $650\text{ }^{\circ}\text{C}$  for 3 h. The G7 and G8 samples were cryo-treated at  $-196\text{ }^{\circ}\text{C}$  for 24 h and 36 h, respectively, before aging after quenching.

Cryogenic treatment was performed by MMD Technology, with the parameters shown in Table 1 with the unit shown in Fig. 1. In the cryogenic treatment, since rapid cooling or heating can cause distortions and material damage, the heating and cooling process was controlled with a nitrogen supply controller. Cooling and heating were carried out by a controller at a rate of  $1\text{ }^{\circ}\text{C}/\text{min}$ .

The heat treatments applied to the samples are given in Fig. 2 as a temperature–time diagram. The materials were machined before the heat treatment procedure. Cryogenic treatment was applied as a deep cryogenic treatment in a liquid nitrogen environment at  $-196\text{ }^{\circ}\text{C}$  and shallow cryogenic treatment at  $-80\text{ }^{\circ}\text{C}$  in a gas nitrogen environment. All samples were subjected to cryogenic treatment and were tempered for 3 h at  $170\text{ }^{\circ}\text{C}$ . Cryogenic treatment soaking time and temperatures were determined in literature studies (Ref 19) and preliminary trials.

The procedure of the aging process is determined by taking into consideration the recommendations of aging parameters from different sources. The samples were heated to  $\alpha + \beta$  region ( $920\text{ }^{\circ}\text{C}$ ) for the solution and held at this temperature for 1 h considering the sample sizes. After the solution treatment,

the samples were quenched to room temperature in the oil medium. Cryogenic treatment was performed after solution treatment before aging as a deep cryogenic treatment for 24 h and 36 h within 24 h following the solution treatment. Then, all samples were aged for 3 h at  $650\text{ }^{\circ}\text{C}$ .

## 2.2 Sample Preparation for Microstructure Analysis and XRD Tests

In order to perform microstructural and XRD, analysis samples were cut prior to heat treatment. Since processing sheet metal samples might be tricky, microstructural investigations were conducted on a cylindrical rod. A silicon carbide (SiC) disk was used to cut the Ti6Al4V bar by using a water-based coolant to minimize the effect of generated heat during the process. The surface of the samples has been prepared by automatic grinding and polishing device. Grinding was performed using emery papers with a mesh of 220, 600 grid. Since the titanium surface can be easily scored, an additional fine grinding was done with 1200 and 2400 emery paper. A 15-N load was applied to each sample in each stage of grinding. The force was generated by the pneumatic unit. In each grinding level, the samples were ground for 10 min. The polishing process was performed with a long-haired pad, and a  $3\text{-}\mu\text{m}$  diamond solution was used. Polished samples were etched with Kroll's agent.

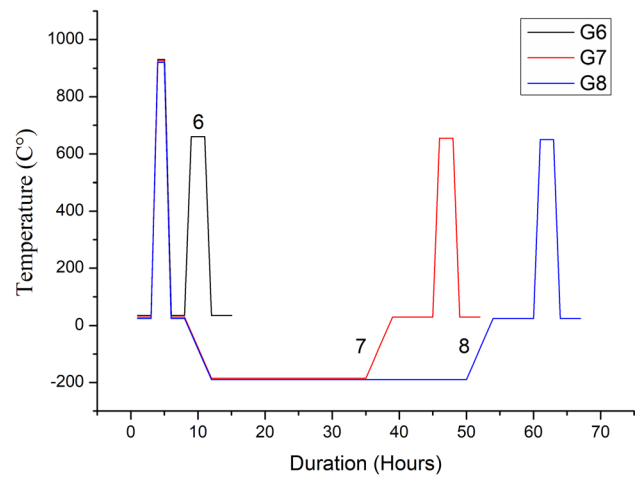
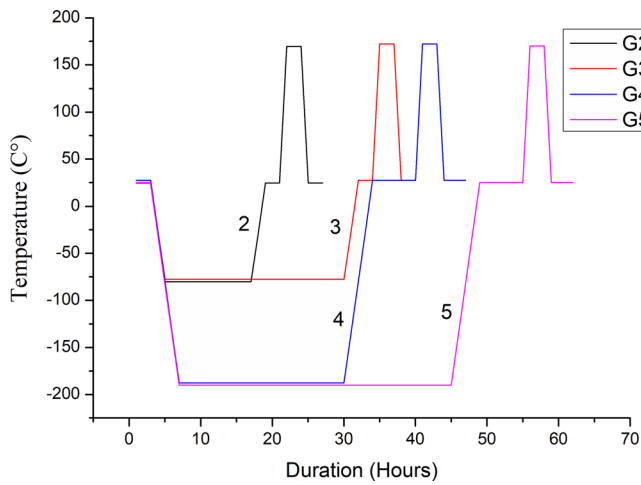
Additionally, another set of samples was prepared for XRD analysis. These samples were also cut from cylindrical rod material with SiC cutting disk and prepared similar to samples



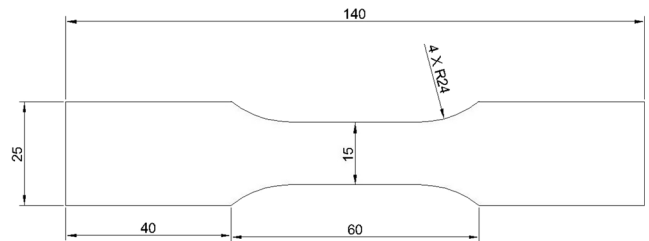
Fig. 1 Cryogenic Treatment Unit, (a) cryo-treated (b) cryo-treated and aged

Table 1 The heat treatment procedure of groups

	Heat Treatment Procedure
G1	As supplied (Annealed at $700\text{ }^{\circ}\text{C}$ )
G2	Cryo-treated at $(-80\text{ }^{\circ}\text{C})$ 12 h, 3-hour tempering at $170\text{ }^{\circ}\text{C}$
G3	Cryo-treated at $(-80\text{ }^{\circ}\text{C})$ 24 h, 3-hour tempering at $170\text{ }^{\circ}\text{C}$
G4	Cryo-treated at $(-196\text{ }^{\circ}\text{C})$ 24 h, 3-hour tempering at $170\text{ }^{\circ}\text{C}$
G5	Cryo-treated at $(-196\text{ }^{\circ}\text{C})$ 36 h, 3-hour tempering at $170\text{ }^{\circ}\text{C}$
G6	Solution treatment at $920\text{ }^{\circ}\text{C}$ 1 h, quenching, 3-h aging at $650\text{ }^{\circ}\text{C}$
G7	Solution treatment at $920\text{ }^{\circ}\text{C}$ 1 h, quenching cryo-treated at $(-196\text{ }^{\circ}\text{C})$ 24 h, 3-h aging at $650\text{ }^{\circ}\text{C}$
G8	Solution treatment at $920\text{ }^{\circ}\text{C}$ 1 h, quenching cryo-treated at $(-196\text{ }^{\circ}\text{C})$ 36 h, 3-h aging at $650\text{ }^{\circ}\text{C}$



**Fig. 2** Temperature time graph



**Fig. 3** Tensile test specimens and dimensions

examined under an optical microscope. The specimens were mounted on the table of a Panalytical ZETIUM x-ray device. All samples were tested under the same conditions. Taking into consideration the studies in the literature, the scanning range was determined between  $25^\circ$  and  $90^\circ$ . The XRD results were analyzed by comparing the patterns; additionally, MAUD software was used to conduct Rietveld analysis. FWHM (full width half maximum) values of XRD peaks of this study were calculated with Origin Pro software.

### 2.3 Tensile Tests

Tensile testing is one of the most commonly used methods to determine the mechanical properties of materials. Sample preparation for tensile testing can be carried out in different directions considering the anisotropy state that may exist in the material structure. These tests can also be carried out at different tensile speeds and ambient temperatures, considering the working conditions of the material. Tensile test specimens of this study were prepared from 1-mm-thick Ti6Al4V sheet material. All samples were cut in the direction of the rolling with the dimensions shown in Fig. 3. The WEDM method was used, and all the samples were cut in a single setup with the same parameters. Geometrical dimensions and sample surface quality were also checked before testing.

The main parameters in the tensile test are sample size to be tested, test temperature, and test speed. The tensile test operates with the principle of drawing a sample from a fixed end at a constant speed in a controlled environment and temperature by recording the required amount of load, and the corresponding elongation is recorded. Performing the tests at different temperatures and different strain rates seriously affect the character of the tensile curve. In this study, tensile tests were

carried out in a universal testing device (Shimadzu AG-IS 250 kN) at room temperature. The tensile speed was determined to be 3 mm/min and kept constant throughout the test. These conditions were chosen to represent the low-speed forming and static loading conditions. The thickness of the samples was 1 mm, and the width of the section was 15 mm, so the sectional area ( $A$ ) was  $15 \text{ mm}^2$ , and the gauge length ( $G$ ) was set as 22 mm. The gauge length was marked symmetrically to the center of the sample.

Different materials show different tensile curve characteristics. The tensile stress diagram obtained by the tensile test can be divided into the elastic region, uniform plastic deformation region (UPDR), and nonuniform plastic deformation region. An exemplary drawing diagram is given in Fig. 4. In this diagram, the horizontal axis shows the strain ( $\epsilon$ ), and the vertical axis shows the stress ( $\sigma$ ).

Toughness and uniform plastic deformation area areas were also calculated with the help of the data obtained from the tests. The toughness and UPDR values of the samples were calculated according to Eq 1 and 2 from the beginning of the experiment until the fracture of the specimen. The integration was carried out numerically.

$$\text{Toughness} = \frac{A}{G} \int_0^{\epsilon_f} \sigma d\epsilon \quad (\text{Eq 1})$$

$$\text{UPDR} = \frac{A}{G} \int_{\epsilon_{yp}}^{\epsilon_{uts}} \sigma d\epsilon \quad (\text{Eq 2})$$

Tensile testing is one of the methods used to observe the formability of materials. In order to obtain good formability without shrinking or tearing of the sheet metal, there are some



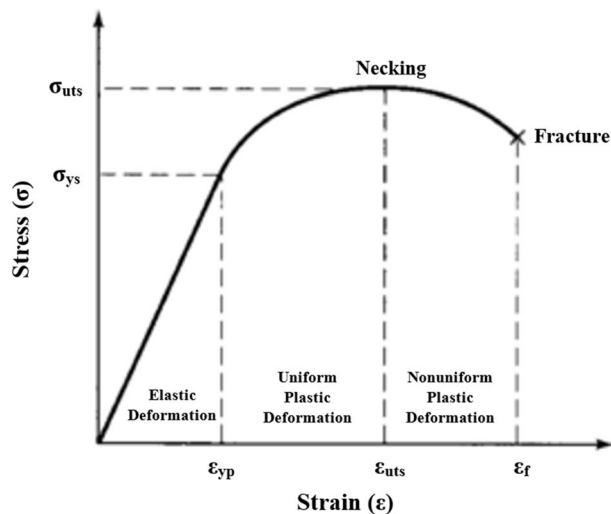


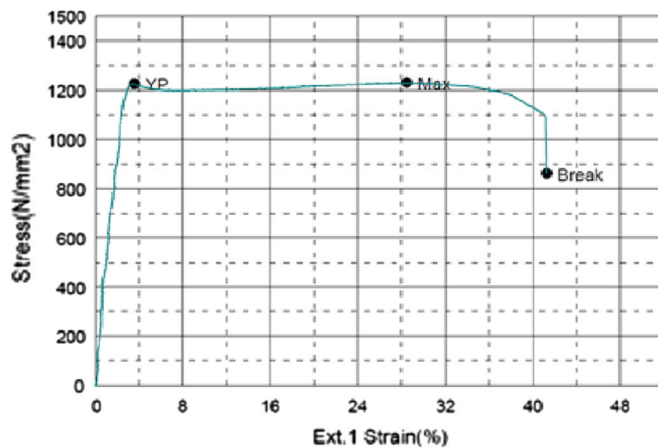
Fig. 4 Tensile test graph schematic and actual graphs

points that can be monitored by analyzing the stress–strain diagram. Firstly, the fluctuation of the load at the yield point is an undesired thing; a smooth transition is desired. Secondly, a large and stable uniform plastic deformation region (UPDR) is desired. Because it is challenging theoretically to predict the exact point where the fracture occurs. After the maximum load, the point has been exceeded in the tensile test; the deformation character becomes a nonuniform state. This region is called a nonuniform plastic deformation region. It is desirable that the UPDR, which is the region between the yield and ultimate tensile strength points where the plastic deformation is uniform, to be as large as possible. In this study, a UPDR area was calculated as a measure of plastic forming ability. Stress and strain points obtained experimentally were used in the calculation. The portion between the yield and ultimate tensile strength points was taken. The area under this section was calculated by taking a numerical integral with Origin Lab Pro software.

### 3. Results and Discussions

#### 3.1 Microstructure and XRD Tests

The investigation of the microstructure of cryo-treated groups shows that there was not a significant change in the overall view of microstructure. Hence, solution treatment and aging changed the form of the  $\beta$  phase structure. The  $\beta$  phase was formed a basket-like form. The microstructure of Ti6Al4V alloy consists of the  $\beta$  phase dispersed in the  $\alpha$  phase matrix. The shape and amount of the  $\beta$  phase significantly affect many properties of the alloy. The main factor that determines the  $\beta$  phase ratio is annealing temperature. However, applying cryogenic treatment affects the ratio of the  $\beta$  phase, either. In this study, two different methods were used to determine the ratio of the  $\beta$  phase in the microstructure. The first method is image processing (IP) of microstructures with 1000X magnification. The second method was the XRD analysis. Figure 5 shows the microstructures taken with 1000X magnification. In order to quantify the amounts of  $\beta$  phase, a free image processing software (ImageX) was used. The samples with different microstructures were etched, and microstructures were



obtained under similar conditions. Since the supplied alloy was annealed at 700 °C, the expected ratio of the  $\beta$  phase was 8.1%. The parameters of image processing were calibrated to obtain the expected  $\beta$  phase ratio. The calibrated parameters were also used to quantify the amount of  $\beta$  phases in other samples. Figure 8 shows the amount of  $\beta$  phases for different heat-treated groups. These results indicate that holding Ti6Al4V alloy at deep cryogenic temperatures alters the  $\beta$  phase amount and leads to the formation of the  $\alpha$  phase. In the aged samples, the solution treatment conducted at the  $\alpha + \beta$  phase region increased the amount of  $\beta$  phase compared to untreated samples. Conducting additional cryogenic treatment to these samples also reduces the amount of the  $\beta$  phase and contributes to the transformation of the  $\beta$  phase to the  $\alpha$  phase.

The second method used to quantify the amount of  $\beta$  phase in the structure was XRD. X-ray diffraction is another way to demonstrate the changes in the internal structure of the material by the effect of cryogenic treatment. The surface analyzed by this method was selected in the same direction as the surface analyzed using the optical microscope. XRD analysis was prepared from cylindrical rod samples to take measurements from the center of the slices cut with a precision cutting disk. The XRD peaks obtained from the samples are plotted in the same graph in Fig. 6. The lattice parameters calculated with Rietveld analysis are also given in Fig. 6.

The XRD peaks give valuable information about surface integrity, residual stress amount, and grain structure (Ref 9). In microstructure analysis, it was determined that the  $\beta$ - $\alpha$  phase transformation occurred with cryogenic treatment by analyzing microstructure images taken from optical microscope and phase analysis. In addition to the phase analysis conducted with the image processing technique, the peaks obtained in XRD measurement were analyzed. For this purpose, XRD patterns of samples were measured. To compare these patterns, CIF (Crystallography information File) files obtained from the literature are provided for all phases that might be present in the structure. MAUD software was used for Rietveld analysis by using CIF files. For possible phases, CIF files were analyzed in the literature. The CIF files used in this study were produced with the help of PDF-4 + 2018 software. In Fig. 7, individual XRD patterns are given for all samples, and Rietveld fitting patterns are given. According to the results of the Rietveld

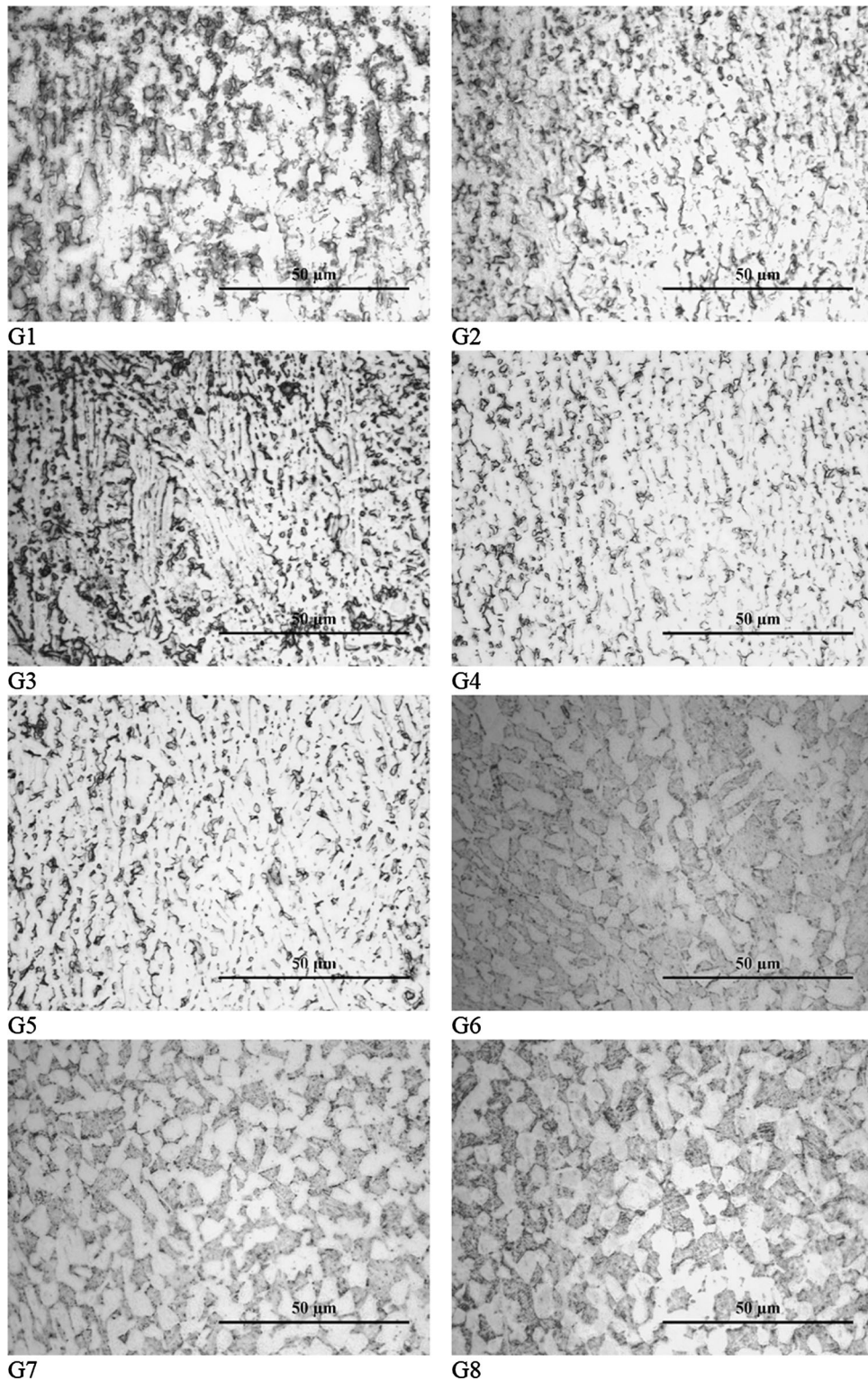
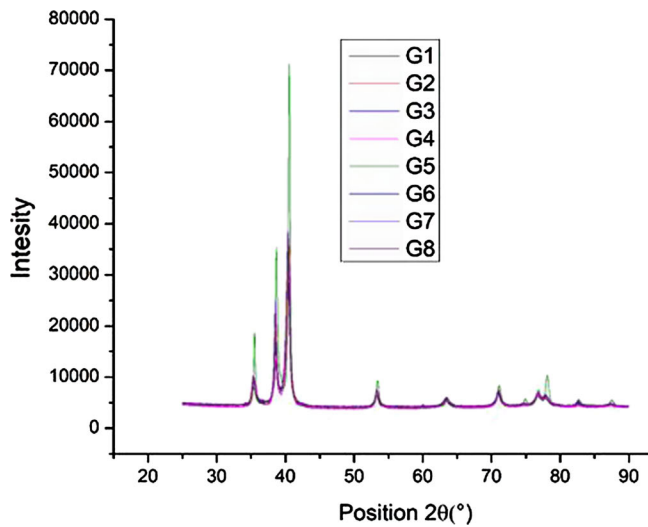


**Fig. 5** Microstructure images of samples (1000X)

analysis and IP,  $\beta$  phase ratios for different samples are presented in Fig. 8.

In addition to the analysis of XRD patterns using Maud software, the changes in the peaks were also analyzed by the overlapping of the peaks individually and comparatively with the peaks of the reference sample. Figure 9 shows the XRD patterns of G1 and G4 samples with peaks drawn on top of each

other. When this figure is examined, it is seen that the peaks belonging to the fourth group widen according to the peaks of the reference group and shifted slightly to the right. In particular, the decrease in intensity at the dominant  $\beta$  peak at  $38^\circ$  supports the findings related to the transformation of the  $\beta$  phase. At the peaks of  $35^\circ$ ,  $42^\circ$ , and  $63^\circ$ , where the alpha phase is dominant, the intensity of the peaks increased, expanded, and



Group No	$\alpha(\text{\AA})$		$\beta(\text{\AA})$
	a	c	
G1	2.9386	4.6671	3.3019
G2	2.9307	4.6668	3.2907
G3	2.9324	4.6652	3.2943
G4	2.9290	4.6719	3.2905
G5	2.9284	4.6523	3.2958
G6	2.9338	4.6692	3.2990
G7	2.9345	4.6675	3.3005
G8	2.9304	4.6646	3.2941

Fig. 6 XRD patterns and lattice parameters of samples

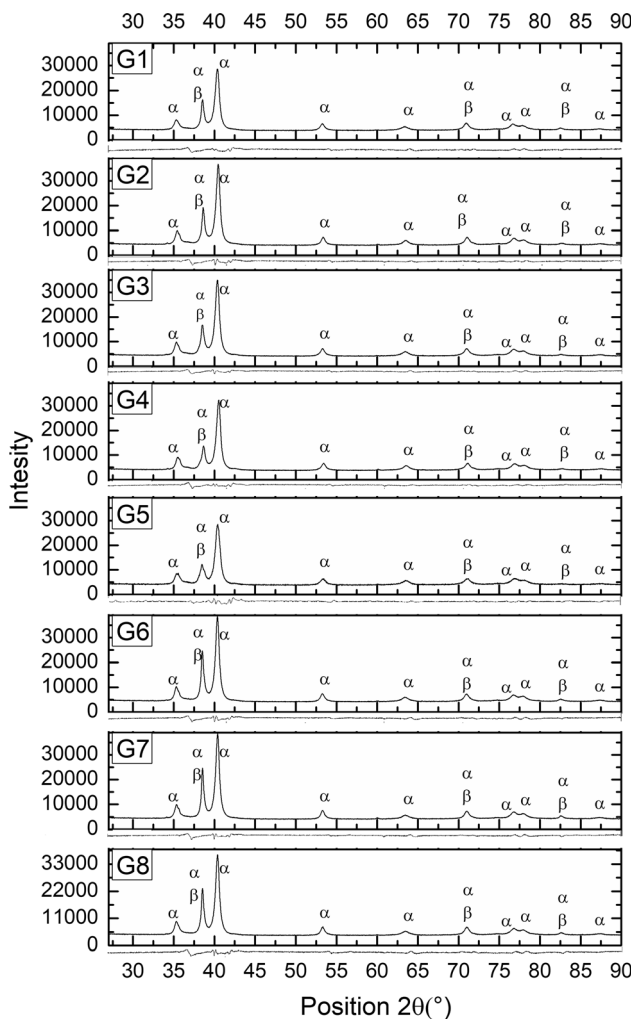


Fig. 7 XRD patterns and Rietveld fitting patterns of samples

shifted slightly to the right. These observations show that the increase in the  $\alpha$  phase ratio and the grains are refined. The shifts of the peaks indicate that the internal stresses in the structure decrease and the structure becomes more stable. The

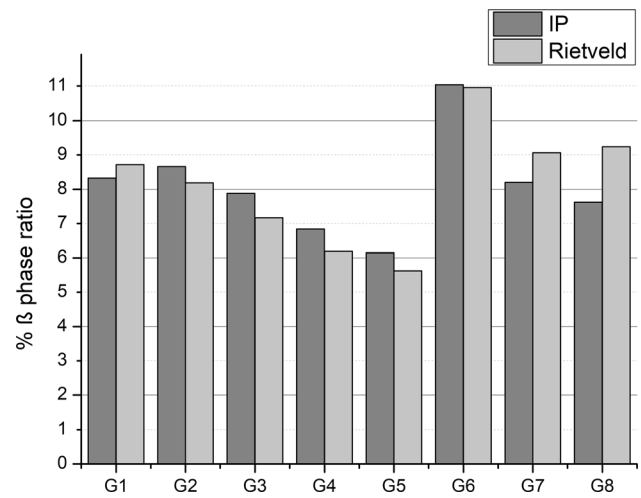


Fig. 8  $\beta$  phase ratios, according to image processing and Rietveld analysis

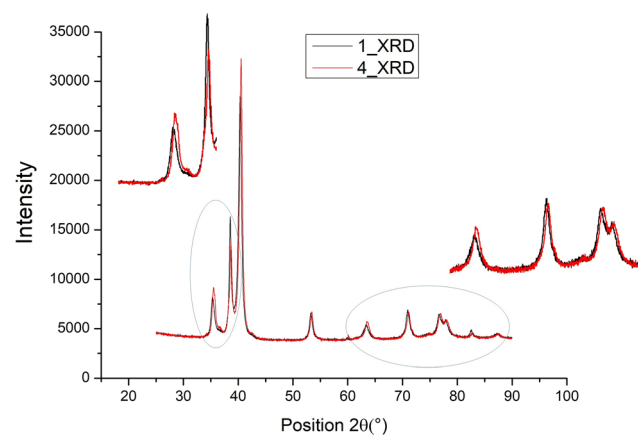


Fig. 9 XRD patterns of G1 and G4

changes observed in peaks of cryogenically treated samples relative to the reference sample were more limited in shallow cryogenic treated samples but more evident in deep cryogenic



treated samples. In addition to these findings observed in XRD analysis, the cryogenic treatment increases the twinning mechanism (Ref 25), decreases residual stress amount, improves electrical conductivity in materials by regulating dislocations (Ref 26), and it has also been reported that there is a significant effect on removal of residual stresses (Ref 27).

XRD analysis of the group 5 also shows  $\beta$  to  $\alpha$  phase transformation. The intensity of peaks dominated by the  $\beta$  phase was decreased. When XRD analyses of group 4 and group 5 were compared, the effect of increased cryogenic treatment time and peak widening or shifting effect was not clearly observed. In this context, XRD analysis of group 5 can be said to be very similar to group 4. These results are consistent with the results of the phase analysis conducted with an optical microscope.

In addition to the changes observed in peaks of  $\beta$  and  $\alpha$  phases of the obtained analysis results, changes in FWHM (full width at half maximum) values are useful for understanding the changes in the structure. In the literature, studies are indicating that peak intensities and FWHM values of peaks correlate with some material properties. FWHM measurements give important clues about the condition of materials since they are affected by grain distortion, dislocation density, and residual stress (Ref 28). The increase in grain defects affects the grain structure and causes an increase in FWHM value (Ref 29). The residual tensile stress in the structure leads to an increase in the FWHM value, while the decrease in the harmful residual tensile stress in the structure causes the FWHM values to decrease (Ref 30). According to these studies, it is desirable to decrease the FWHM value. Therefore, all peaks of group 1 and group 4 were analyzed, and FWHM values were calculated and are given in

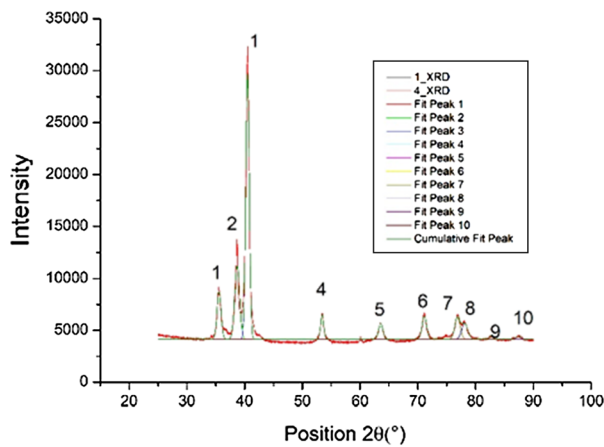


Fig. 10 FWHM values for G1 and G4

Fig. 10. When the values were examined, it was observed in the XRD analysis of group 4 in terms of  $\alpha$  phase that the FWHM values were lower than those of group 1, only the peaks of 2.6 and 9 where  $\beta$  phase was effective. The reason for this increase is that the intensity of the peaks weakens with the decrease in the  $\beta$  phase. Although the  $\alpha$  phase ratio at the other peaks increased, the decrease is thought to indicate that the structure is regulated, and the amount of residual stress decreases.

XRD patterns of the samples subjected to aging show that the  $\beta$  phase ratio in the structure increased with the aging process. This effect is supported by the intensification of peaks at 38-70 and 83° and Rietveld analysis results where the  $\beta$  phase is effective. Among the aged samples, the application of cryogenic treatment just after quenching decreased the  $\beta$  phase ratio slightly compared to the sample treated with aging. When the XRD patterns of group 6 and group 8 were examined, it was observed that the peak intensities in which the  $\beta$  phase was effective decreased, but the effect of grain widening and grain rearrangement observed only in cryogenically treated samples was not dominant in the aged treated samples. The results are also consistent with the studies in the literature (Ref 31). Similarly, the positions of the peaks did not change significantly. Therefore, it can be said that the effect of cryogenic treatment conducted after the solution treatment on residual stress and dislocation density in the internal structure is more limited compared to the samples treated with cryogenic treatment alone. According to XRD results, the application of cryogenic treatment after quenching affects the phase ratios of aging samples, but it is thought that the aging process plays a more dominant role in determining the crystallographic properties.

	FWHM 1	FWHM 4
Peak1	0,89733	0,83417
Peak2	0,71206	1,0016
Peak3	0,77022	0,71773
Peak4	0,63672	0,63851
Peak5	0,9746	0,8849
Peak6	0,90573	0,93062
Peak7	1,06886	1,08319
Peak8	1,28913	1,22086
Peak9	0,66798	0,67439
Peak10	0,95696	0,98813



### 3.2 Tensile Tests

In the tensile test, for the experimental validity of test results, all of the tests were repeated for at least three times for each group. Results are given on average values, and deviation amounts are shown as error bars. A tensile test was carried out at the universal testing device (Shimadzu AG-IS 250 kN) at Eskişehir Osmangazi University Metallurgical Institute at room temperature and at low speed (3 mm/min) to represent static conditions. The gauge length was determined as 22 mm, considering the sample dimensions and marked on the samples. These signs were monitored by the camera system on the device, and calculations are made automatically by the computer. The tensile test was performed in three replicates for eight groups in which different procedures were applied, and average results are given in Table 2. Additionally, among all tested samples, the ones that were close to the average values of groups were chosen, and a tensile curve for all samples is given in Fig. 11.

According to the tensile test results, approximately 5% yield strength and 4% tensile strength improvement was achieved in the samples subjected to the aging process. Cryogenically treated samples showed a decrease in yield strength of less than 2%. Toughness and plastic forming capability was calculated numerically as depicted in section 2.3. When the plasticity and toughness properties were examined, it was observed that cryogenic treatment provided a significant improvement, especially in the fourth and fifth groups, which were cryo-treated at  $-196\text{ }^{\circ}\text{C}$ . According to this calculation, it was observed that the UPDR of the samples applied for 36-h deep cryogenic treatment increased by 8.3%. It was observed that the samples treated with deep cryogenic treatment for 24 h achieved a 5% improvement. According to these results, deep cryogenic treatment of Ti6Al4V alloys increased plastic forming ability and toughness according to tensile tests conducted at room temperature. As expected, the aging process showed a 20% decrease in toughness. The application of deep cryogenic treatment after the solution in the aging process has enabled the material to recover some of its lost plasticity (3%). Although the cryogenic treatment before the aging process compensated some of this decrease in toughness, no significant improvement was observed as much as in groups 4 and 5. The graphical results of tensile tests and error bars are given in Fig. 12.

Although the effect of the cryogenic treatment is thought to be related to the dimensions of the sample being tested and its effect may decrease as the thickness of the specimen's increase, it can be said that 24–36 h of deep cryogenic treatment can be effective to improve the plastic forming properties of sheet

materials. It can be noted that the results of tensile tests are consistent with previous studies in the literature (Ref 1). Besides, sample sizes and properties that can be obtained by tensile testing are consistent with the information in the literature (Ref 32). When the titanium alloys are examined, it is seen that in general, it is preferable to form at temperatures between 200 and 400  $^{\circ}\text{C}$  close to the annealing temperature depending on the material condition where cold forming is not preferred. Examples of cold-formed titanium alloys are grade 1, the  $\alpha$ -titanium alloy. The improvement in toughness and plasticity provided by the cryogenic process can be associated with regulated dislocations and residual stress reduction in the internal structure. This effect had some negative effect on the material strength of the grain boundaries and caused a decrease in yield strength of the materials by 2%. This effect is more pronounced in samples treated with deep cryogenic treatment for 36 h compared to samples treated with deep cryogenic treatment for 24 h.

During deep cryogenic treatment of Ti6Al4V alloy, the temperature of the material gradually decreases to  $-196\text{ }^{\circ}\text{C}$ . At a temperature this low; a considerable volumetric thermal shrinkage occurs inside the material. This shrinkage also causes compression of lattice structures at the molecular level. This compression effect is observed in the lattice structure level; this phenomenon occurs more dominantly in the  $\beta$  phase, which has a BCC lattice structure rather than the  $\alpha$  phase with the HCP lattice structure, where molecular movements are more difficult.

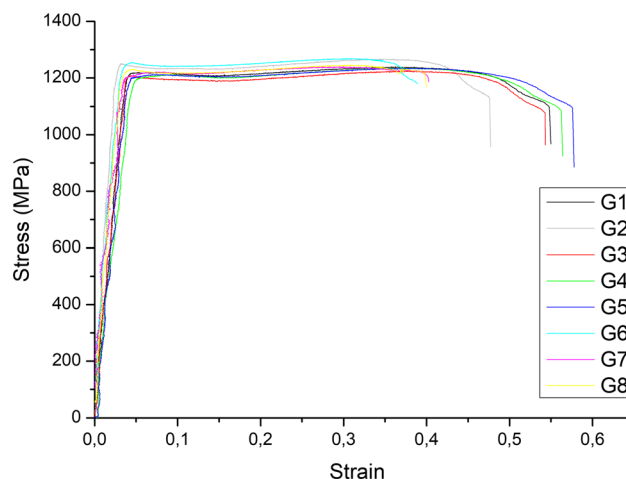
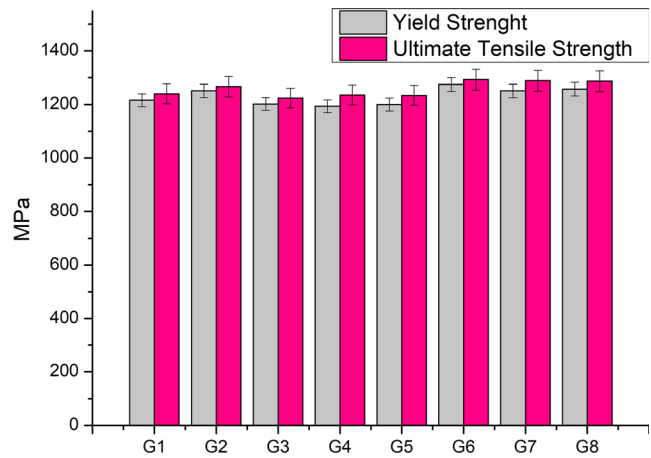
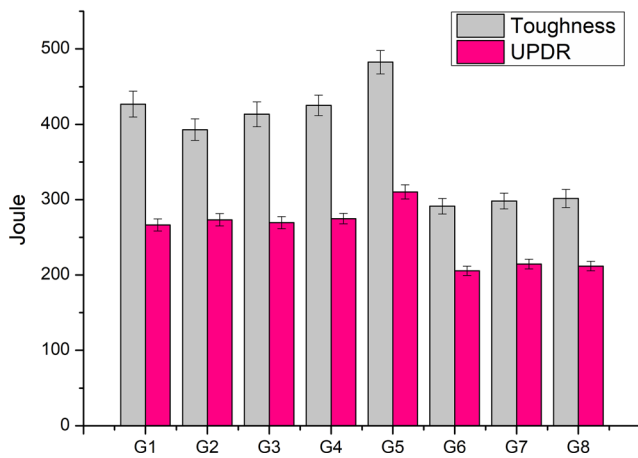


Fig. 11 Stress-strain graph of samples

Table 2 Average results of tensile tests

	Yield Strength, MPa	Yield strength strain, %	Ultimate tensile strength, MPa	Ultimate strength strain, %	Break strain, %	Toughness, J	UPDR, J
1	1216	4.0	1240	36.2	54.9	424	265
2	1251	4.1	1266.67	34.4	47.7	383	266
3	1202	4.4	1224.48	36.9	54.3	415	270
4	1194	4.6	1235.94	38.6	56.4	430	278
5	1200	4.4	1234.38	38.7	57.8	445	286
6	1274	4.8	1292.79	30.9	39.3	288	204
7	1251	4.8	1288.45	31.8	40.3	295	213
8	1258	4.7	1286.83	32.0	40.6	299	210



**Fig. 12** Tensile test results

This compression effect promotes the movement of atoms at the atomic level. With the effect of the atomic movements at the molecular level, the unstable  $\beta$  phase transforms into stable  $\beta$  phase and  $\alpha$  phase. Dislocations are rearranged to a less energy state and became balanced, and it is thought that micro-deformations occur and that decrease internal stresses.

The observed improvement in tensile tests and characterization studies show that deep cryogenic treatment affects the overall performance of Ti6Al4V alloy. The main observed effect was the transformation of the  $\beta$  phase to the  $\alpha$  phase. The authors of the paper think that the theory of the mechanism behind this transformation is strongly related to the vanadium element, a  $\beta$  stabilizer alloying element of Ti6Al4V alloy. The cryogenic treatment is performed at sub-zero temperatures about  $-196\text{ }^{\circ}\text{C}$ , that kind of a low temperature causes volumetric shrinkage of material and lattice structures. The  $\beta$  phase that has a BCC lattice structure shrinks as well. As the soaking time increases, the V atoms in the structure begin to diffuse. The  $\beta$  phase loses some of its vanadium element, which is a  $\beta$  stabilizer. Since the  $\beta$  phase does not have enough stabilizers cannot remain in the  $\beta$  phase and transform into the  $\alpha$  phase. Since the  $\alpha$  matrix can only dissolve a limited amount of V element, the undissolved V element travels to the semi-stable  $\beta$  phase, and as it finds more  $\beta$  stabilizer, the semi-stable  $\beta$  phase transforms to stable  $\beta$ . Since the diffusion is too low at low temperatures, this process takes long durations. For enough shrinkage of BCC lattice, too low temperatures are required. A recent study about the topic is to point out a similar theory (Ref 33)

## 4. Conclusion

The experimental studies and analysis show that cryogenic treatment of Ti6Al4V alloy causes many changes in materials properties. Since cryogenic treatment is a kinematic process, the duration and temperature of cryogenic treatment are effective on the experimental results. The microstructural and XRD analysis showed that with the application of cryogenic treatment internal structure of material changed, some amount of  $\beta$  phase transformed into  $\alpha$  phase, the internal stresses in the structure decreased, and the grains were refined. For the 24-h and 36-h deep cryo-treated samples, the  $\beta$  phase ratio was

measured as 5.6 and 6.2%, while reference samples  $\beta$  phase ratio was measured as 8.1%. Tensile tests were performed to observe the effects of cryogenic treatment on the formability of Ti6Al4 alloys and to determine the effect of the mechanical properties. According to the results of these tests, it was observed that the cryogenic treatment had a positive influence on the plasticity properties of Ti6Al4V alloy. For the 24-h and 36-h deep cryo-treated samples, the UPDR was extended 5 and 8.3%, respectively. However, this improvement in plasticity observed in samples treated with cryogenic treatment for 36 h led to a decrease in yield strength by 2%. The aging process applied to Ti6Al4 V alloys is a known strengthening mechanism. It has been determined by experimental studies that the aging process increases yield strength by about 5% but decreases toughness about 30% and plasticity about 20%. The application of deep cryogenic treatment after the solution in the aging process has enabled the material to recover some of its lost plasticity (3%). The effects of cryogenic treatment are much more dominant in lower operating temperatures, shallow ( $-80\text{ }^{\circ}\text{C}$ ) cryogenic treated samples also showed  $\beta$ - $\alpha$  transformation, but this effect is more pronounced in deep ( $-196\text{ }^{\circ}\text{C}$ ) cryogenic treated samples. Therefore, the effect of shallow cryogenic treatment on the structure is limited. The results showed that deep cryogenic treatment helps to transform unstable  $\beta$  phases to  $\alpha$  phase and stable  $\beta$  phase, lowers internal stress and improves mechanical properties and formability of Ti6Al4 alloy.

## Acknowledgment

This work was supported by a research program supported by the Eskisehir Osmangazi University, Project Number 2017/15A210.

## References

1. K. X. Gu, J. J. Wang, Z. Yuan, H. Zhang, Z. Q. Li, and B. Zhao, Effect of Cryogenic Treatment on the Plastic Property of Ti-6Al-4V Titanium Alloy, 2014, pp. 42–47, <https://doi.org/10.1063/1.4860602>
2. K.X. Gu et al., The Effect of Cryogenic Treatment on the Microstructure and Properties of Ti-6Al-4V Titanium Alloy, *Mater. Sci. Forum*, 2013, **747–748**, p 899–903. <https://doi.org/10.4028/www.scientific.net/MSF.747-748.899>

3. W. Sha and S. Malinov, *Titanium alloys: modelling of microstructure, properties and applications*, CRC Press, Boca Raton, 2009
4. L. Zeng and T.R. Bieler, Effects of Working, Heat Treatment, and Aging on Microstructural Evolution And Crystallographic Texture of  $\alpha$ ,  $\alpha'$ ,  $\alpha''$  and  $\beta$  Phases in Ti-6Al-4V Wire, *Mater. Sci. Eng. A*, 2005, **392**(1–2), p 403–414. <https://doi.org/10.1016/j.msea.2004.09.072>
5. Y.-G. Huang, J.-R. Chen, M.-L. Zhang, X.-X. Zhong, H.-Q. Wang, and Q.-Y. Li, Electrolytic Boronizing of Titanium in  $\text{Na}_2\text{B}_4\text{O}_7$ -20% $\text{K}_2\text{CO}_3$ , *Mater. Manuf. Process.*, 2013, **28**(12), p 1310–1313. <https://doi.org/10.1080/10426914.2013.840912>
6. J.W. Elmer, T.A. Palmer, S.S. Babu, and E.D. Specht, In Situ Observations of Lattice Expansion and Transformation Rates of  $\alpha$  and  $\beta$  Phases in Ti-6Al-4 V, *Mater. Sci. Eng. A*, 2005, **391**(1–2), p 104–113. <https://doi.org/10.1016/j.msea.2004.08.084>
7. R. Singh, A. Kurella, and N.B. Dahotre, Laser Surface Modification of Ti-6Al-4V: Wear and Corrosion Characterization in Simulated Biofluid, *J. Biomater. Appl.*, 2006, **21**(1), p 49–73. <https://doi.org/10.1177/0885328206055998>
8. P. Singh, H. Pungotra, and N.S. Kalsi, Optimization of Deep Cryogenic Treatment Conditions for the Wear Rate Of UNS R56400 (Ti6Al4V) Medical Titanium Alloy using Taguchi's Method, *Mater. Technol.*, 2019, **34**(2), p 84–91. <https://doi.org/10.1080/10667857.2018.1523099>
9. J.I. Qazi, O.N. Senkov, J. Rahim, and F.H. (Sam) Froes, Kinetics of Martensite Decomposition in Ti-6Al-4V-xH Alloys, *Mater. Sci. Eng. A*, 2003, **359**(1–2), p 137–149. [https://doi.org/10.1016/s0921-5093\(03\)0350-2](https://doi.org/10.1016/s0921-5093(03)0350-2)
10. M.T. Jovanović, S. Tadić, S. Zec, Z. Mišković, and I. Bobić, The Effect of Annealing Temperatures and Cooling Rates on Microstructure and Mechanical Properties of Investment Cast Ti-6Al-4V Alloy, *Mater. Des.*, 2006, **27**(3), p 192–199. <https://doi.org/10.1016/j.matdes.2004.10.017>
11. B. Callegari et al., In-situ Synchrotron Radiation Study of The Aging Response of Ti-6Al-4V Alloy with Different Starting Microstructures, *Mater. Charact.*, 2020, **165**, p 110400. <https://doi.org/10.1016/j.matchar.2020.110400>
12. B. Callegari et al., New Insights into the Microstructural Evolution of Ti-5Al-5Mo-5V-3Cr Alloy During Hot Working, *Mater. Charact.*, 2020, **162**, p 110180. <https://doi.org/10.1016/j.matchar.2020.110180>
13. I. Gunes, A. Cicek, K. Aslantas, and F. Kara, Effect of Deep Cryogenic Treatment on Wear Resistance of AISI, 52100 Bearing Steel, *Trans. Indian Inst. Met.*, 2014, **67**(6), p 909–917. <https://doi.org/10.1007/s12666-014-0417-4>
14. A. Çiçek, F. Kara, T. Kivak, E. Ekici, and İ. Uygur, Effects of Deep Cryogenic Treatment on the Wear Resistance and Mechanical Properties of AISI, H13 Hot-Work Tool Steel, *J. Mater. Eng. Perform.*, 2015, **24**(11), p 4431–4439. <https://doi.org/10.1007/s11665-015-1712-x>
15. F.H. Çakir and O.N. Çelik, Improvement of the Machinability of Ti-6Al-4V Alloy Wire Electro Discharge Machining with Cryogenic Treatment, *Met. Mater. Int.*, 2020, <https://doi.org/10.1007/s12540-020-00667-z>
16. N.A. Özbek, Effects of Cryogenic Treatment Types on the Performance of Coated Tungsten Tools in the Turning of AISI, H11 Steel, *J. Mater. Res. Technol.*, 2020, **9**(4), p 9442–9456. <https://doi.org/10.1016/j.jmrt.2020.03.038>
17. E. Nas and N. Altan Özbek, Optimization of the Machining Parameters in Turning of Hardened Hot Work Tool Steel using Cryogenically Treated Tools, *Surf. Rev. Lett.*, 2020, **27**(05), p 1950177. <https://doi.org/10.1142/s0218625x19501774>
18. D. Mohan Lal, S. Renganarayanan, and A. Kalanidhi, Cryogenic Treatment to Augment Wear Resistance of Tool and Die Steels, *Cryogenics*, 2001, **41**(3), p 149–155. [https://doi.org/10.1016/s0011-275\(01\)00065-0](https://doi.org/10.1016/s0011-275(01)00065-0)
19. F.H. Çakir and O.N. Çelik, The Effects Of Cryogenic Treatment on the Toughness and Tribological Behaviors of Eutectoid Steel, *J. Mech. Sci. Technol.*, 2017, **31**(7), p 3233–3239. <https://doi.org/10.1007/s12206-017-0613-3>
20. Y. Yao, X. Li, and X. He, *Effect of Deep Cryogenic Treatment on Mechanical Properties and Microstructure of Sn3.0Ag0.5Cu Solder*, *J. Sci. Mater. Electron. Mater.*, 2017, <https://doi.org/10.1007/s10854-017-8400-6>
21. S.J. Gobbi, V.J. Gobbi, G. Reinke, P.V. Muterlle, and D.M. Rosa, Ultra-low-Temperature Process Effects on Microscale Abrasion of Tool Steel AISI, D2, *Mater. Sci. Technol.*, 2019, **35**(11), p 1355–1364. <https://doi.org/10.1080/02670836.2019.1624018>
22. Z. Hu, C. Guo, and H. Li, Influence of AZ31 Sheet Treated by Cryogenic on Punch Shearing, *J. Cent. South Univ.*, 2019, **26**(6), p 1582–1591. <https://doi.org/10.1007/s11771-019-4114-7>
23. A. Sert and O.N. Celik, Characterization of the Mechanism of Cryogenic Treatment on the Microstructural Changes in Tungsten Carbide Cutting Tools, *Mater. Charact.*, 2019, **150**, p 1–7. <https://doi.org/10.1016/j.matchar.2019.02.006>
24. S. Kalia, Cryogenic Processing: A Study of Materials at Low Temperatures, *J. Low Temp. Phys.*, 2010, **158**(5–6), p 934–945. <https://doi.org/10.1007/s10909-009-0058-x>
25. K. Gu, B. Zhao, Z. Weng, K. Wang, H. Cai, and J. Wang, Microstructure Evolution in Metastable  $\beta$  Titanium alloy Subjected to Deep Cryogenic Treatment, *Mater. Sci. Eng. A*, 2018, **723**, p 157–164. <https://doi.org/10.1016/j.msea.2018.03.003>
26. D. S. Nadig, V. Ramakrishnan, P. Sampathkumaran, and C. S. Prashanth, “Effect of cryogenic treatment on thermal conductivity properties of copper,” Spokane, Washington, USA, 2012, pp. 133–139, <https://doi.org/10.1063/1.4712089>
27. K. Gu, J. Wang, and Y. Zhou, Effect of Cryogenic Treatment On Wear Resistance of Ti-6Al-4V Alloy for Biomedical Applications, *J. Mech. Behav. Biomed. Mater.*, 2014, **30**, p 131–139. <https://doi.org/10.1016/j.jmbbm.2013.11.003>
28. M. Vashista and S. Paul, Correlation Between Full Width at Half Maximum (FWHM) of XRD Peak with Residual Stress on Ground Surfaces, *Philos. Mag.*, 2012, **92**(33), p 4194–4204. <https://doi.org/10.1080/14786435.2012.704429>
29. H.-M. Tung, J.-H. Huang, D.-G. Tsai, C.-F. Ai, and G.-P. Yu, Hardness and Residual Stress in Nanocrystalline ZrN Films: Effect of Bias Voltage and Heat Treatment, *Mater. Sci. Eng. A*, 2009, **500**(1–2), p 104–108. <https://doi.org/10.1016/j.msea.2008.09.006>
30. S. Rai, B.K. Choudhary, T. Jayakumar, K.B.S. Rao, and B. Raj, Characterization of Low Cycle Fatigue Damage in 9Cr-1Mo Ferritic Steel using x-ray Diffraction Technique, *Int. J. Press. Vessels Pip.*, 1999, **76**(5), p 275–281. [https://doi.org/10.1016/S0308-0161\(98\)0014-0-9](https://doi.org/10.1016/S0308-0161(98)0014-0-9)
31. K.-X. Gu, K.-K. Wang, J.-P. Zheng, L.-B. Chen, and J.-J. Wang, Electrochemical Behavior of Ti-6Al-4 V Alloy in Hank's Solution Subjected to Deep Cryogenic Treatment, *Rare Met.*, 2018, <https://doi.org/10.1007/s12598-018-1163-2>
32. ASM International, J. R. Davis, and ASM International, Eds., *Heat treating*, [10. ed.], 8. print. Materials Park, Ohio: ASM International, 2007
33. K.-X. Gu, K.-K. Wang, J.-P. Zheng, L.-B. Chen, and J.-J. Wang, Electrochemical Behavior of Ti-6Al-4V Alloy in Hank's Solution Subjected to Deep Cryogenic Treatment, *Rare Met.*, 2018, <https://doi.org/10.1007/s12598-018-1163-2>

**Publisher's Note** Springer Nature remains neutral with regard to jurisdictional claims in published maps and institutional affiliations.